UCRL-JC-133454
PREPRINT

Theory of the Equation of State of Hot Dense Matter

M. P. Surh
T. W. Barbee III
L. H. Yang

This paper was prepared for submittal to the
International Conference on High Pressure Science and Technology
Honolulu, Hawaii
July 25 - 30, 1999

July 23, 1999

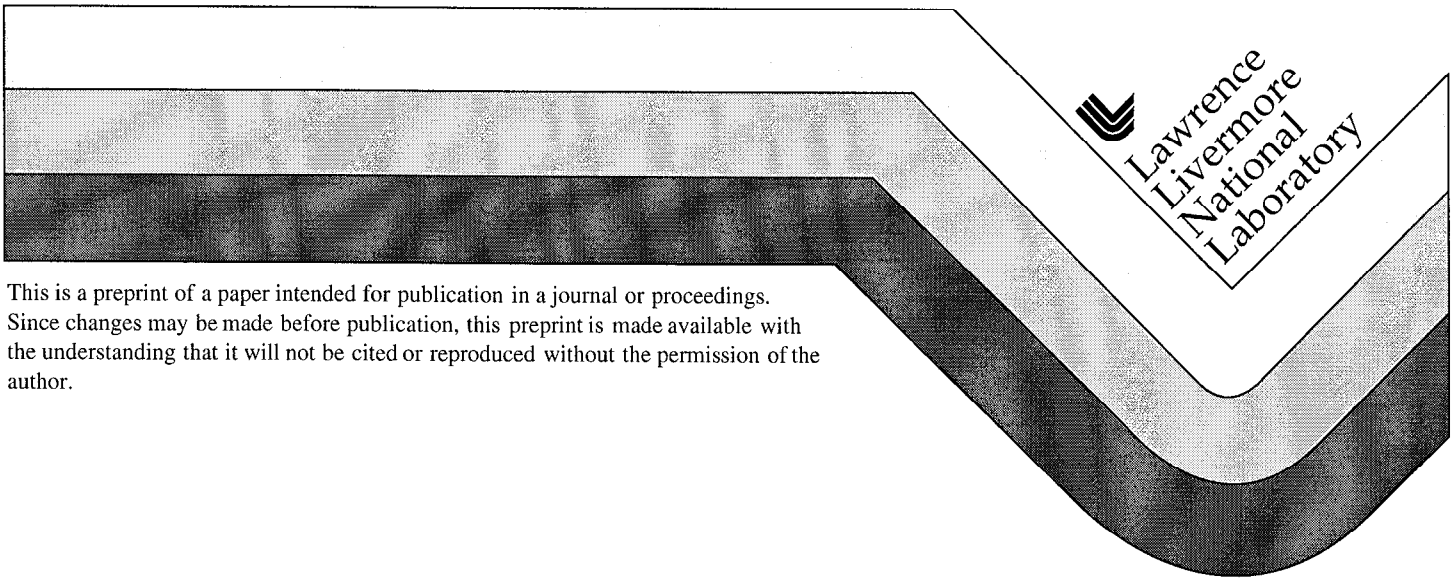

Theory of the Equation of State of Hot Dense Matter

Michael P. Surh, T.W. Barbee III, and L.H. Yang

Lawrence Livermore National Laboratory
Mail Stop L-45
P.O. Box 808
Livermore, California 94551

Ab initio molecular dynamics calculations are adapted to treat dense plasmas for temperatures exceeding the electronic Fermi temperature. Extended electronic states are obtained in a plane wave basis by using pseudopotentials for the ion cores in the local density approximation to density functional theory. The method reduces to conventional first principles molecular dynamics at low temperatures with the expected high level of accuracy. The occurrence of thermally excited ion cores at high temperatures is treated by means of final state pseudopotentials. The method is applied to the shock compression Hugoniot equation of state for aluminum. Good agreement with experiment is found for temperatures ranging from zero through 10^5K. [equation of state, aluminum, molecular dynamics simulation, first principles, shock Hugoniot]

Numerous theoretical methods exist to compute equilibrium properties of matter at either low or high temperatures. For example, the molecular dynamics (MD) technique has achieved widespread use in condensed matter theory for the study of both solid and liquid properties. In *ab initio* versions, the ions move classically while electrons are treated quantum mechanically in the Born-Oppenheimer adiabatic approximation. Often, it is a satisfactory approximation to take the electronic system to have zero temperature ($T_{ele} = 0, T_{ion} > 0$), although this restriction is not required (1, 2, 3). Plasma theories are applicable at high temperatures, especially for $k_B T >> E_F$, where the electronic system becomes increasingly classical in character. However, little theoretical progress has been made in the intermediate temperature regime, where both ion-electron and ion-ion correlations may have significant temperature dependence. A fully quantum mechanical treatment of the electrons is necessary here along with the inclusion of multiple electron-ion scattering at the lower range. (For example, this gives rise to pair or bond-angle correlations in liquids and, ultimately, to long range order in the solid phase.) These requirements motivate an effort to extend condensed matter theory calculations to higher temperatures.

Standard *ab initio* MD employs the local density approximation (LDA) to Hohenberg-Kohn-Sham density functional formalism (4). The calculations commonly use either fictitious electron dynamics or iterative schemes to keep electrons near the Born-Oppenheimer equilibrium state. Forces on the atoms are obtained by the Hellmann-Feynman theorem (1). Typical calculations with electron temperature $T_{ele} = 0$ may be improved by using the Mermin formalism for the independent-particle contribution to electronic entropy (5), which requires populating states according to the Fermi-Dirac distribution of the Kohn-Sham eigenlevels. Reliable free energies also require a temperature dependent exchange and correlation potential; here, the parametrization of Tanaka and Ichimaru will be used (6) in addition to the Ceperley and Alder zero temperature results (7, 8).

Such a generalization of conventional *ab initio* MD can be applied to high temperatures, $T > T_F$, provided that an all-electron calculation is performed. In many condensed systems, shallow core levels lie 10-50 eV below the top of the valence band (9); the core orbitals form narrow bands of Bloch states for periodic boundary conditions. Clearly, these levels must be partially unoccupied at temperatures in excess of 10^4 K.

However, most practical *ab initio* MD calculations are performed with a norm-conserving pseudopotential approximation, which allows the practical use of a plane wave basis set. The pseudopotential relies on a rigid core approximation (i.e., the core orbitals and occupations are assumed to be identical to the ground state of the free atom). Not only does thermal core ionization violate this assumption, but thermally excited conduction electrons penetrate the core and screen the Coulomb potential of the nucleus. This reduces the binding energy of core levels, and gives rise to so-called continuum lowering as a function of temperature and density (10, 11). Finally, pseudopotential calculations are also problematic whenever core orbitals overlap at extreme pressure or temperature. Therefore, it is necessary to relax the rigid core constraint in order to use pseudopotential methods at high temperature. One approach is to construct an Al pseudopotential for the L-shell electrons, i.e., with an ion charge of $Z = +11$. However, this is not practical for large-scale MD simulations in a plane wave basis.

Recently, first principles pseudopotential theory has been successfully applied to the study of photoemission (12, 13, 14, 15). Separate calculations are made for atomic pseudopotentials with a photoexcited core hole and a correspondingly increased ionic charge. It is assumed that the core hole has a long lifetime such that the neighboring electrons fully respond to the perturbation. The modified pseudo-ion is then treated as a defect in a standard pseudopotential calculation of the solid surface or bulk. By choosing fictitious core hole dynamics, it is possible to extend this method to systems with thermally excited ion cores in the plasma state. This is a felicitous approximation for plane wave LDA studies, as the excited core pseudopotentials are similar to the original aluminum.

In general, multiply ionized core configurations will occur

Table 1. Total energies in Ry for the constrained DFT of neutral Al versus L- and M-shell occupations. The K-shell is fully occupied in all cases. Self-consistent LDA energies are obtained using the Perdew-Zunger zero temperature exchange and correlation. They are obtained for spherically symmetric charge distributions; for example, the energy difference between two $2p_x$ holes and a $2p_x$ plus $2p_y$ combination is neglected. The mean core occupations and total energies for the 144,000K and 300,000K pseudopotentials are shown at the bottom. The minor core ionization that occurs at lower temperatures is neglected.

Orbital Occupations	Total Energy (Ry)	Core Degeneracy
$2s^2 2p^6 3s^2 3p^1$	0.000	1
$2s^2 2p^5 3s^2 3p^2$	5.522	6
$2s^1 2p^6 3s^2 3p^2$	8.217	2
$2s^2 2p^4 3s^2 3p^3$	12.252	15
$2s^1 2p^5 3s^2 3p^3$	14.864	12
$2s^0 2p^6 3s^2 3p^3$	17.062	1
$2s^{2.000} 2p^{5.986} 3s^2 3p^{1.014}$	0.069*	
$2s^{1.977} 2p^{5.727} 3s^2 3p^{1.296}$	2.276†	

* T=144,000K mean atomic configuration
† T=300,000K mean atomic configuration

at high temperatures (see Table I). It is necessary to estimate the equilibrium concentrations of ion core species as a function of density and temperature. This is a difficult task, since interionic and electronic correlations may play a role in determining the chemical equilibrium among the different species. However, if the effect of interionic interactions is neglected in determining species concentrations, the problem becomes a matter of the equilibrium distribution of a single ion in an electron plasma. Density functional calculations for such ion-plasma systems have been performed in the past (16, 17).

Here, the energies of *isolated*, neutral atoms are calculated for varying excited core configurations and shown in Table I. The temperature-dependent ion concentrations, n_i, are subsequently obtained from the partition function

$$n_i = -\frac{1}{\beta}\partial \ln Z/\partial \varepsilon_i; \quad Z = \sum_i e^{-\beta \varepsilon_i} \tag{1}$$

in terms of $\beta = 1/k_B T$, total atomic energies, ε_i, and the degeneracies of the atomic configurations, i. This estimate neglects the effect of continuum lowering on the ion core energies, and so the predicted n_i are independent of density. This approximation should be acceptable for moderate temperatures and densities, where the error is expected to be small compared to the core hole creation energies.

The atomic total energies in Table I are obtained in a so-called constrained density functional method (18). That is, they are not the energies of a ground state or free energies of systems in thermodynamic equilibrium. This constrained DFT has the advantage of including some portion of the core hole-core hole Coulomb interactions in the calculated energies for multiply excited atoms. For example, the energy of the doubly ionized core energy is not simply twice that of a singly ionized configuration. This may mark an improvement over the average atom approximation, which assumes a Fermi-Dirac distribution according to the atomic Kohn-Sham eigenvalues (16).

Once the relative ion concentrations are determined, thermodynamic equilibrium among the ion cores must be established by molecular dynamics. (The free electrons are always in equilibrium at a temperature T_{ele}.) In the absence of dynamical core-hole transitions, this model is essentially one of a non-stoichiometric fluid alloy. In this case, the alloy is primarily composed of Al with small admixtures of Si-, P-, S-, and Cl-like final state pseudoatoms accounting for singly through four-fold ionized cores. There are numerous techniques available for the study of alloy systems. By far, the simplest scheme is the virtual crystal approximation (VCA), which averages the different (non-local) ionic pseudopotentials (19) according to their concentrations, n_i, to yield a single, ion potential:

$$V^{VCA}_{pseud}(r, r') = \sum_i n_i V^i_{pseud}(r, r') \tag{2}$$

A VCA-like approach is taken here (20), for MD calculations of solid or fluid aluminum at temperatures, $T_{ele} = T_{ion}$, of 0; 3,000; 10,000; 30,000; 75,000; 144,000; and 300,000K. Pseudopotentials are calculated using the method of Troullier and Martins (21) from a single core configuration of average 2s and 2p orbital occupation numbers that are obtained from the partition function in Eq. 1 and the atomic energies from Table I. Aluminum L-shell cores are essentially unperturbed until T =144,000K, at which point the average ion has 0.014 core holes ($\langle Z \rangle = 3.014$). At 300,000K, the ion has an average of 3.296 elementary charges (22).

Plane wave pseudopotential calculations are performed for a cubical unit cell at fixed volume and containing 32 aluminum atoms. The single Γ-point is used for Brillouin zone sampling. The plane wave basis is cut off at 15 to 25 Ry and includes a total of approximately 900 basis functions at the highest densities. The number of valence electrons is adjusted to maintain charge neutrality when the mean ion charge, $\langle Z \rangle$, varies with temperature. At the highest temperature of 300,000K, 850 bands are included for a spectrum of eigenvalues that spans approximately 180 eV. This allows a reasonable approximation to the correct Fermi-Dirac distribution at $k_B T_{ele} = 25.85$eV. The electron chemical potential is self-consistently determined so as to give the correct total number of electrons for the limited spectrum of eigenvalues.

A time step of 6 atomic units (1.45×10^{-16} s) is used to perform molecular dynamics by Verlet integration. This time step is an order of magnitude smaller than for typical *ab initio* MD calculations. However, the temperatures used here are as much as two orders of magnitude higher than considered in the past, which makes the average atomic displacements between successive time steps comparable to previous studies. The atomic

coordinates are started from a well equilibrated ensemble, and the atomic velocities are given a Maxwellian distribution appropriate to the desired temperature, $T_{ion} = T_{ele}$. The ionic temperature fluctuates as the total kinetic energy varies during time evolution of the system, $\frac{3}{2}N_{ion}k_B\langle T_{ion}\rangle = \langle U_{ion}^{kin}\rangle$. If the calculated ionic temperature instantaneously differs from the desired value by more than 10%, the atomic velocities are rescaled to the desired temperature. Ionic pressure contributions are given as $\langle P_{ion}\rangle = N_{ion}k_B\langle T_{ion}\rangle/V$. Electronic pressures are obtained from the Hellmann-Feynman stress tensor. The volume, V, and statistical average temperature and pressure, $\langle T\rangle$ and $\langle P\rangle$ yield the predicted equation of state.

For example, MD simulations can readily identify a shock Hugoniot for aluminum. The Hugoniot is a locus of points (densities and pressures) for equilibrium states that can be achieved by successively stronger shocks from a given reference state. (The experimental starting state for aluminum at ambient pressure and temperature is 2.7 g/cm^3 density.) Experimental Hugoniot data exists from gas gun measurements and nuclear detonations (23, 24, 25, 26, 27, 28, 29, 30). The Hugoniot is identified theoretically from conservation laws to satisfy the relation:

$$[U - U_0] - [(P + P_0)(V_0 - V)]/2 = 0 \qquad (3)$$

in terms of internal energy, U; pressure, P; and volume, V. The subscript 0 denotes the initial conditions; these quantities are also obtained by LDA calculations. Known, small LDA errors in density and cohesive energy do not appreciably alter the predicted Hugoniot. Calculations are made for a range of densities (volumes) and for a fixed average temperature.

The internal energy of the ground state is calculated as:

$$U_{solid} = U_{solid}^{pseudo} + U_{atom}^{all-elec} - U_{atom}^{pseudo} \qquad (4)$$

in terms of calculated energies for the isolated atom with all electrons (including the core), $U_{atom}^{all-elec}$, and for the free atom and solid with just the valence electrons (using the pseudopotential), U_{atom}^{pseudo} and U_{solid}^{pseudo}, respectively. This result depends on the transferrability properties of norm-conserving pseudopotentials; namely, that the cohesive energy is correctly given by $E_{cohes} = E_{solid}^{pseudo} - E_{atom}^{pseudo}$ Similarly, the internal energy of an instantaneous atomic configuration of the hot, dense plasma in the Born-Oppenheimer approximation is:

$$U_{plasma} = U_{plasma}^{pseudo} + U_{atom}^{all-elec} - U_{atom}^{pseudo} + U_{ion}^{kin} \qquad (5)$$

using the pseudopotential appropriate to the given temperature.

The expectation values of internal energy and pressure must be computed from the MD simulations by statistical sampling. Averages and error bars are estimated by sampling data every 20 time steps and assuming the complete absence of serial correlation. In this case, the RMS error is given as $\sigma/\sqrt{N}$ in terms of the calculated variance, σ, and number of samplings, N. Residual serial correlation in the sampling creates a slight underestimate in the error bars. Up to 1000 timesteps are taken with careful convergence of wavefunctions and energies. More time steps taken with looser tolerances give similar results. Sample results for the Hugoniot relation are shown in Fig.

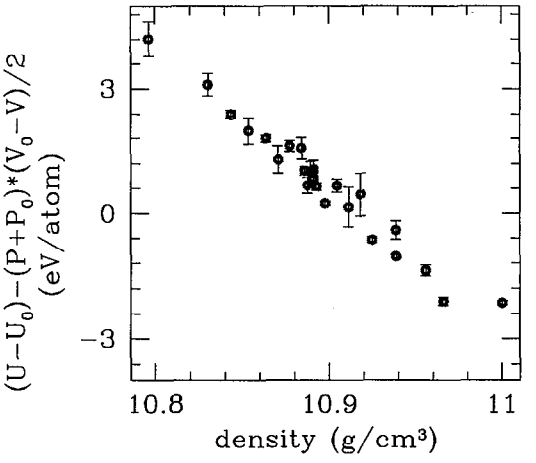

FIGURE 1. Comparison of the Hugoniot relation versus density for T=300,000K. These calculations are performed with final state pseudopotentials with average core occupation numbers appropriate to this temperature. A dense set of points versus volume was chosen to aid in analysis. Simulations at other temperatures were limited to a few points around the estimated Hugoniot density.

1. Statistical fluctuations are minimized by averaging the difference $\langle [U - U_0] - [(P + P_0)(V_0 - V)/2]\rangle$, rather than taking the difference of the averages $\langle [U - U_0]\rangle - \langle [(P + P_0)(V_0 - V)/2]\rangle$.

Core ionization has a significant effect on the predicted Hugoniot through several mechanisms. First, some portion of the energy delivered by the shock is absorbed when ionizing core levels. Therefore, the temperature of the system is lower than would otherwise develop. Second, the total number of free particles increases as the ion cores partially dissociate. Third, the ionic charge is increased by the partial ionization, which alters the ion-ion Coulomb repulsion. Fourth, the ion cores contract in the presence of core holes, reducing the short range overlap repulsion of the cores. Fifth, the usual, filled shell core repulsion is modified by core hole hybridization and polarization. (These last two effects are not currently included in this pseudopotential calculation. Core repulsion must be incorporated either as a pair-potential correction or as a tight-binding fit to all electron calculations.)

The combined influence of the first three of these effects can be seen in Fig. 2, which shows the predicted Hugoniot for fixed occupation Al pseudopotentials (Z=3) and for the final state pseudopotentials with average core level occupations. The three Al valence electrons are always fully delocalized, so the $Z = 3$ model system has zero ionization energy and never exceeds the infinite shock limit of four-fold compression. In contrast, the final state pseudopotential calculation includes the effect of increasing core ionization with temperature. This re-

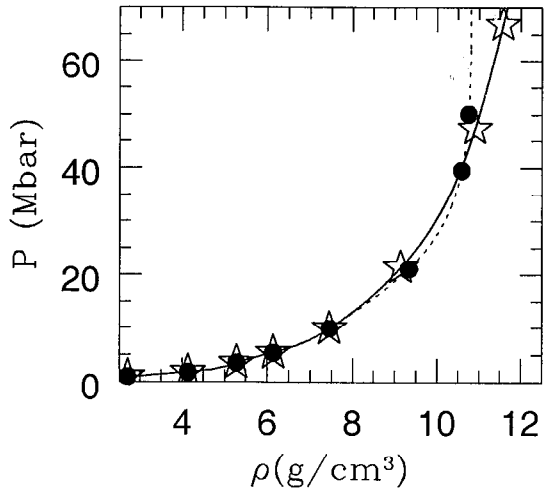

FIGURE 2. Comparison of Al Hugoniot as calculated by *ab initio* MD using filled-core, fixed occupation pseudopotentials, Z=3.0, (filled circles and dashed curve) and using mean thermal occupation final state pseudopotentials (stars and solid curve). The zero temperature exchange and correlation potential are used here. Results are displayed for temperatures of 0, 3×10^3, 11.6×10^3, 30×10^3, 75×10^3, 144×10^3, 300×10^3, and 400×10^3 K. The lines are cubic spline fits to guide the eye. The two curves will asymptotically meet at four-fold compression of the starting state for infinite shocks and infinite temperature.

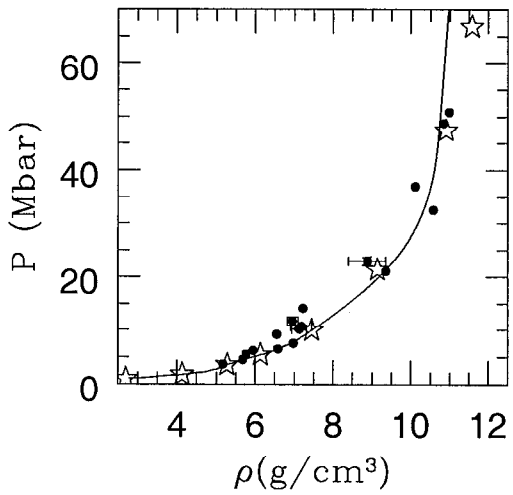

FIGURE 3. Comparison of the MD Hugoniot using final state pseudopotentials (star symbols) to experimental data from Refs. (23, 24, 25, 26, 27, 28, 29, 30) (filled circles). Representative experimental error bars are shown, where available. The solid curve is a spline fit to the calculations.

duces the predicted temperatures versus shock strength and allows compression to significantly higher densities.

Agreement between the final state pseudopotential MD results and experiment appears good, as seen in Fig. 3. Statistical uncertainties in the MD results are comparable to the sizes of the symbols displayed. The LDA calculations give slight errors in the density and cohesive energies at ambient conditions, and in the predicted melting point of aluminum (3, 31). However, these errors have little effect on the Hugoniot on the scale of Fig. 3.

A comparison of MD and earlier theoretical equations of state is shown in Fig. 4. It is likely that the positioning of the MD results between the two earlier theories and in proximity with the experiment is partly accidental. All of the theoretical curves displayed are considered to be in agreement with the experimental results, given the uncertainties in the shock measurements. The MD results also lack two important corrections at this time. There is no continuum lowering in the calculation for the ion core configurations. This will lower the ionization energy for core holes, and should bring closer agreement with the ACTEX result (32). There is also no contribution to the calculated pressure or internal energy from the overlap of adjacent ion cores. This repulsion will yield a less compressible system, in closer accord with the Livermore Al equation of state table (33). Finally, the MD calculations are performed with an exchange and correlation potential for the zero temperature electron gas. The effect of a finite temperature electron gas exchange and correlation potential is shown as a single $\times$ symbol for T=300,000K. This is only a correction to the zero temperature result, taken from calculations for the electron gas at the given temperature and density.

In summary, first principles molecular dynamics calculations are applied to the equation of state of shock compressed aluminum for the first time. The method used for low temperatures (below 10,000K) is typical of *ab initio* MD calculations. Key approximations include Born-Oppenheimer, LDA, and the use of norm-conserving pseudopotentials. Temperatures below 100,000K require the addition of the Mermin formalism for electronic free energy and a finite-T exchange and correlation. Finally, the recently developed final state pseudopotential method based on constrained DFT is used for still higher temperatures, ranging to 400,000K. This pseudopotential scheme is combined with the virtual crystal approximation to complete a molecular dynamics model for disordered, non-stoichiometric mixtures of ions. The results are in good agreement with experiment, and work is underway to incorporate further modifications to the pseudopotential method (?) in order to apply it to dense plasmas at yet higher temperatures.

The authors acknowledge G. Galli, D.A. Young, F.J. Rogers, B.I. Bennett, and A. Hazi for helpful discussions on this problem. This work was performed under the auspices of the U.S. Department of Energy by Lawrence Livermore National Laboratory under Contract No. W-7405-Eng-48.

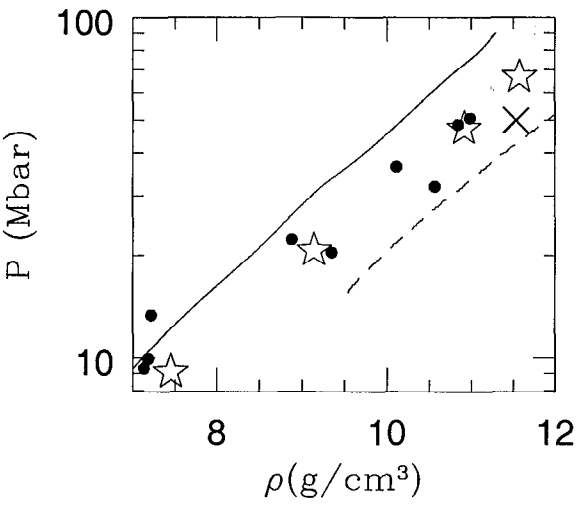

FIGURE 4. Comparison of the high pressure MD Hugoniot using final state pseudopotentials (star symbols) to experimental data from Refs. (23, 24, 25, 26, 27, 28, 29, 30) (filled circles) and to the theoretical Hugoniot from the tabulated Livermore Al equation of state (33) (solid line) and from calculations with the ACTEX method (32) (dashed line). MD results are shown for T= 75×10^3, 144×10^3, 300×10^3, and 400×10^3 K. The average ion charge at these temperatures is 3.0, 3.014, 3.296, 3.571, respectively. A single $\times$ symbol represents a calculation at 300×10^3K with a finite-T exchange and correlation correction for the itinerant electrons.

References

1. R.M. Wentzcovitch, J.L. Martins, and P.B. Allen, Phys. Rev B **45**, 11372 (1992).
2. M.P. Grumbach, D. Hohl, R.M. Martin, and R. Car, J. Phys. Cond. Matt. **6**, 1999 (1994).
3. G.A. de Wijs, G. Kresse, and M.J. Gillan, Phys. Rev. B **57**, 8223 (1998).
4. P. Hohenberg and W. Kohn, Phys. Rev. **136**, B864 (1964), and W. Kohn and L.J. Sham, Phys. Rev. **140** A1133)1965).
5. N.D. Mermin, Phys. Rev. **137**, A1441 (1965).
6. S. Tanaka and S. Ichimaru, Phys. Rev. B **39**, 1036 (1989).
7. D.M. Ceperley and B.J. Alder, Phys. Rev. Lett. **45**, 566 (1980).
8. J.P. Perdew and A. Zunger, Phys. Rev. B **23** 5048 (1981).
9. (For comparison, occupied valence band widths or Fermi energies are typically 10-20 eV.)
10. M.W.C. Dharma-Wardana and F. Perrot, Phys. Rev A **45**, 5883 (1992).
11. D. Liberman and J. Albritton, J. Quant. Spectrosc. Radiat. Transfer **51**, 197 (1994).
12. E. Pehlke and M. Scheffler, Phys. Rev. Lett. **71**, 2338 (1993).
13. J.-H. Cho, S. Jeong, and M.-H. Kang, Phys. Rev. B **50**, 17139 (1994).
14. A. Pasquarello, M.S. Hybertsen, and R. Car, Phys. Rev. B **53**, 10942 (1996).
15. A. Catellani, G. Galli, and F. Gygi, Phys. Rev. Lett. **77**, 5090 (1996).
16. D.A. Liberman, Phys. Rev. B **20**, 4981 (1979), and J. Quant. Spectrosc. Radiat. Transfer **27**, 335 (1982).
17. F. Perrot and M.W.C. Dharma-Wardana, Phys. Rev. E **52**, 5352 (1995).
18. A.K. McMahan, R.M. Martin, S. Satpathy, Phys. Rev. B **38**, 6650 (1988).
19. T. Soma, Y. Funuyama, H.M. Kagaya, Sol. St. Comm. **77**, 149 (1991).
20. Core level transitions are expected to be frequent at high densities, in which case MD with the mean core level occupations may give a better approximation to the true ion trajectories than with a collection of different pseudoions with fixed charge $Z = +3, +4, +5$, etc.
21. N. Troullier, and J.L. Martins, Phys. Rev. B **43**, 1993 (1991).
22. The mean orbital occupations are weighted by the atomic *total energies* so that the result is distinct from the usual average atom approximation.
23. L.V. Al'tshuler, N.N. Kalitkin, L.V. Kuz'mina, and B.S. Chekin, Zh. Eksp. Teor. Fiz. **72**, 317 (1977).
24. A.C. Mitchell, W.J. Nellis, J.A. Moriarty, R.A. Heinle, N.C. Holmes, R.E. Tipton, and G.W. Repp, J. Appl. Phys. **69**, 2981 (1991). A.P. Volkov, N.P. Voloshin, A.S. Vladimirov, N.N. Nogin, and V.A. Simonenko, Pis'ma Zh. Eksp. Teor. Fiz. **31**, 623 (1980).
25. C.E. Ragan III, Phys. Rev. A **25**, 3360 (1982).
26. A.S. Valdimirov, N.P. Voloshin, V.N. Nogin, A.V. Petrovtsev, and V.A. Simonenko, Pis'ma Zh. Eksp. Teor. **39**, 69 (1984).
27. V.A. Simonenko, N.P. Voloshin, A.S. Valdimirov, A.P. Nagibin, V.N. Nogin, V.A. Popov, V.A. Vasilenko, and Yu. A. Shoidin, Zh. Eksp. Teor. Fiz. **88**, 1452 (1985).
28. E.N. Avrorin, B.K. Vodolaga, N.P. Voloshin, V.F. Kuropatenko, G.V. Kovalenko, V.A. Simonenko, and B.T. Chernovolyuk, Pis'ma Zh. Eksp. Teor. Fiz. **43** 241 (1986).
29. E.N. Avronin, B.K. Vodolaga, N.P. Voloshin, G.V. Kovalenko, V.F. Kuropatenko, V.A. Simonenko, and B.T. Chernovolyuk, Zh. Eksp. Teor. Fiz. **93**, 613 (1987).
30. R.F. Trunin, Usp. Fiz. Nauk. **164**, 1215 (1994).
31. J.W. Jong, I.-W. Lee, and K.J. Chang, Phys. Rev. B **59**, 329 (1999).
32. F.J. Rogers, and D.A. Young, Phys. Rev. E **56**, 5876 (1997).
33. D.A. Young, J.K. Wolford, F.J. Rogers, and K.S. Holian, Phys. Lett. **108A**, 157 (1985).